



USE OF FIBRE REINFORCED POLYMER TO ENHANCE THE SLIDING SHEAR RESISTANCE OF UNREINFORCED CONCRETE MASONRY

Frank Campanaro¹ and Robert Drysdale² and Ahmad Hamid³

¹M.A.Sc. Candidate, McMaster University, Hamilton, ON.

²Professor and Martini, Mascarini and George Chair in Masonry Design, McMaster University, Hamilton, ON.

³Professor and Director of the Masonry Research Lab, Drexel University, Philadelphia, PA. Adjunct Professor, McMaster University, Hamilton, ON.

All members of Centre for Effective Design of Structures, McMaster University, Hamilton, ON.

ABSTRACT

An experimental investigation was conducted at the Centre for Effective Design of Structures at McMaster University to study the influence of fibre-reinforced polymer (FRP) laminates on the sliding shear resistance of unreinforced masonry (URM). This paper presents the results from the initial phase of this investigation which involved selection of an appropriate test specimen shape. Thirty-six URM assemblages were tested in direct shear, and of these fourteen were retrofitted with an FRP laminate. Thus, the only test parameters were the shape of the test specimen and the presence of the FRP retrofit. The results showed that the application of FRP laminates on URM greatly improved the shear slip strength, deformation characteristics, and post-peak response. The retrofitted specimens reached shear slip strengths ranging from 3.2 to 7.7 times that of their non-retrofitted counterparts.

KEYWORDS: concrete masonry, FRP, sliding shear, URM

INTRODUCTION

Recently, FRP laminates have been successfully used for seismic retrofitting of URM walls. Structural masonry reinforced with FRP is truly the coming together of the old and new world. While masonry has existed since the beginning of recorded history, FRP is one of the most recent additions to structural engineering rehabilitation. FRP is a composite material composed of high strength fibres, made from carbon, glass or aramid, suspended in an epoxy resin. The epoxy allows for the even distribution of load to all the fibres and protects them from damage. FRP has many desirable properties for structural engineering applications such as a high strength-to-weight ratio, corrosion resistance and fatigue resistance [1]. FRP also has the benefit of being available in virtually unlimited lengths. Therefore, when laminates or fabric strips are adhered to a wall they can be long and continuous.

The need for an effective strengthening technique is apparent when one considers that masonry structures still constitute a significant percentage of the building stock, many of which can be classified as low-rise buildings, having only one or two stories [2]. Unfortunately, a significant number of these structures are situated in seismic regions and were either constructed before

appropriate seismic design provisions were available or do not meet current seismic design requirements. It is typical for these structures to be constructed of brick or block units bonded together by cement mortar with little or no reinforcing steel. In fact, steel reinforced masonry was not introduced in the United States until the 1930s [1]. Lateral loads (either wind or seismic) are resisted primarily by the in-plane strength and stiffness of the walls oriented parallel to the direction of the applied load. The concern associated with relying on these URM shear walls is that the typical mode of failure is characterized by brittle behaviour with rapid decreases in capacity and very limited deformations after reaching the ultimate load. In many low-rise masonry buildings subjected to lateral load, shear is the controlling mode of failure. It is well documented in the literature [3, 4, 5] that the three failure modes associated with the in-plane loading of URM shear walls depend on the combinations of the applied load, wall geometry and properties of the constituent materials. The three failure modes are:

- Tension Controlled/Rocking Failure
- Sliding/Shear Slip Failure
- Diagonal Tension Failure

Shear slip failure is characterized by the relative motion of masonry above and below a mortar bed joint. This failure mode is most likely to occur when both the aspect ratio (height to length) and compressive axial load are relatively low, as is the case with most low-rise buildings. In most cases, the slip failure occurs along the interface between the mortar and the unit rather than through the mortar joint [4]. The capacity of a wall to resist shear-slip, or sliding failure, is a combination of the adhesion and shear-friction resistance between the mortar and the masonry units. Experimental investigations [6, 7] have shown that the shear-slip strength along a mortar joint is composed of the initial shear bond strength between the mortar and the unit, plus the shear-friction capacity due to the vertical load. The following Mohr-Coulomb shear strength relationship is commonly used to model this phenomenon.

$$\tau = \tau_0 + \mu\sigma_n \quad \text{Equation 1}$$

where τ is the total joint shear strength, σ_n is the compressive stress normal to the bed joints, τ_0 is the initial shear bond strength, and μ is the coefficient of friction, which Atkinson et al. [7] reported as ranging from 0.7 to 0.85. However, other research has led to the use of μ equal to 1.0 in Canadian design [8]. The Mohr-Coulomb shear strength relationship assumes that the shear friction capacity is proportional to the applied compressive stress. Experimental investigations [6, 7] have shown that this is the case in the linear elastic region associated with relatively low axial compression.

The potential failure of URM shear walls is further exacerbated in existing buildings when mortar joints have reduced shear capacity due to aging and associated deterioration. The disadvantages of traditional retrofitting and strengthening techniques, such as jacketing with steel-reinforced shotcrete, cast-in-situ concrete, or internal reinforcement, are that they are generally labour intensive and add weight to the structure. Any weight added to the building will alter the inertial forces and hence alter the earthquake response [9]. Furthermore, existing structural elements may be unable to support the additional weight, requiring them to be strengthened as well. This is where the high strength-to-weight ratio of FRP makes its use very appealing.

Research using full scale wall tests to evaluate the effectiveness of FRP reinforcing to resist shear slip would be limited by time and cost considerations. In addition, such tests do not create pure shear conditions so that interpretation of the results is complicated by consideration of more complex stress conditions. It was desirable to be able to conduct a sufficient number of tests to evaluate various FRP reinforcing alternatives and it was desirable to isolate the influence of bed joint shear to facilitate interpretation of the test data. Therefore, a necessary first step in this research was to evaluate various test specimen configurations and to choose the most satisfactory one. In addition, this reported first phase of the research provides some initial insight into the effectiveness of this retrofit method.

LITERATURE REVIEW

Although the utilization of FRP for structural engineering applications is relatively recent, its potential benefits have been recognized and thus significant research has already been reported. A majority of the masonry-related research conducted to date has focused on the out-of-plane behaviour of URM retrofitted with externally applied FRP laminates.

The work done by Ehsani et al. [1] is of particular interest because the results of shear slip tests on URM retrofitted with FRP are reported. Thirty-seven direct shear tests were constructed using three standard clay bricks in a “triplet” type specimen. These specimens were retrofitted with FRP laminates of varying length, density (strength) and fibre orientation (0° & 90° , 45° & 135°). A sheet of lubricated plywood was placed between the bricks so the contribution of the mortar to the shear resistance could be ignored. This was also done to try to simulate the detrimental effect of an initial gap between the bricks on the shear strength. The specimens were tested under displacement controlled, monotonically increasing loading. The two failure modes reported were influenced by the strength and development length of the fabric. The first failure mode was shear failure along one of the bed joints and the second failure mode was delamination of the fabric in the middle brick region or fabric edges (bond failure). For higher fibre density fabrics, the latter debonding failure predominated. Shorter laminates showed combined shear failure as well as delamination. In most cases, the ultimate load of the $45^\circ/135^\circ$ orientated fabric was slightly greater than its $0^\circ/90^\circ$ counterpart at the same fabric density. Also, the displacement at the ultimate load for the $45^\circ/135^\circ$ orientation was 20% to 30% of that for the $0^\circ/90^\circ$ orientation. An almost constant stiffness was observed for the $45^\circ/135^\circ$ FRP throughout the entire loading range. For the $0^\circ/90^\circ$ FRP the stiffness was initially constant but decreased gradually. It was concluded that orienting the fibres at $45^\circ/135^\circ$ will allow the wall to resist larger forces within a smaller amount of deformation, while using $0^\circ/90^\circ$ oriented FRP will produce a more ductile failure at slightly lower loads.

Hamid et al. [10] conducted an investigation to study the influence of FRP on the in-plane behaviour of URM. Forty-two URM assemblages, constructed using one-third-scale “true-model” [11] blocks, were tested under different stress combinations representing the range of stress conditions present in masonry shear and infill walls. Of these 42 assemblages six were 4-block joint shear, or direct shear, specimens. Three of the direct shear specimens were strengthened with a bi-directional $0^\circ/90^\circ$, 0.25 mm thick Glass-FRP (GFRP) sheet with 2.55 g/cm^3 of E-glass fibres bonded to both faces. The joint shear strength of the retrofitted specimens was found to be 8.2 times that of the unretrofitted counterparts. Also, the average slip displacement of the retrofitted specimens was over 34 times that of the unretrofitted counterparts.

The FRP prevented sudden brittle failure associated with shear slip failure and allowed a more gradual ductile failure to occur.

SPECIMEN TYPES AND DESIGNATIONS

In this preliminary investigation, 40 specimens were constructed using standard 20 cm hollow concrete blocks and Type-S mortar. These specimens, as can be seen in Figure 1, are simply modifications of the “triplet” and “modified triplet” used in past studies [4] to determine the shear-slip resistance along mortared bed joints. The modified triple shape provided symmetry about the midheight above and below the gap provided to permit slip.

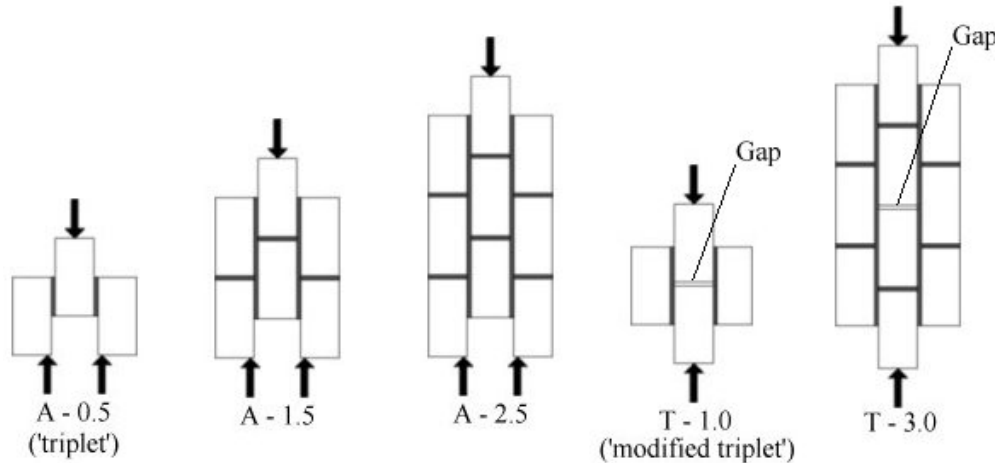


Figure 1 - Test Specimens and Loading Conditions

For later reference, note that the designation for each specimen begins with the letter ‘A’ or ‘T’. The letter ‘A’ indicates the specimen is a ‘triplet’ or a variation of it, and the letter ‘T’ indicates the specimen is a ‘modified triplet’ or a variation of it. The next letter in the designation is ‘U’ or ‘R’ which stand for unreinforced or reinforced, respectively. Reinforced specimens had a bi-directional $0^{\circ}/90^{\circ}$, 0.25 mm thick Glass-FRP (GFRP) sheet with 2.55 g/cm^3 density of E-glass fibres bonded to both faces using epoxy. The next number in the designation indicates the length of the mortared bed joint as a multiple of the number of blocks. The last number is simply the specimen number. Five specimen shapes were selected and eight of each were constructed. Out of each eight specimens only three were reinforced with GFRP. The type of GFRP reinforcement was kept constant so that the performance of each shape could be directly compared. Four specimens were damaged and were not tested.

MATERIAL PROPERTIES

To simulate actual construction practices, Type-S mortar was used to construct the assemblages. The mix proportions by weight were 1 part Portland cement, 0.21 parts lime and 3.53 parts masonry sand. The average compressive strength of the thirty-six 50 mm mortar cubes was 25.1 MPa with a 5.6 % coefficient of variation (COV). The mortar had an average flow of 120.4 % for the 12 batches with a 5.5 % COV. The properties of the GFRP composite were determined according to ASTM D-3039 specifications and were provided by the manufacturer [12]. These properties can be found in Table 1. No independent tests were conducted for the preliminary phase.

Table 1 - GFRP Composite Properties

Composite Laminate Properties	Value
Ultimate tensile strength in primary fibre direction (MPa)	309
Elongation at break (%)	1.6
Tensile Modulus (GPa)	19.3
Ultimate tensile strength 90° to primary fibre direction (MPa)	309
Laminate thickness (mm)	0.25

CONSTRUCTION AND PREPARATION OF THE TEST SPECIMENS

An experienced mason constructed all the specimens in order to minimize the effect of varying workmanship on the properties of the assemblages. The head joints between the two middle blocks of the ‘T’ specimens were left unfilled to allow these specimens to fail in shear-slip. The specimens were allowed to cure for at least 28 days before they were prepared for application of the GFRP. Any excess mortar in the open head joints of the ‘T’ specimens was removed to prevent it from interfering with the relative slip of the blocks along the bed joints. The surfaces of all the specimens were cleaned with a wire brush to remove any deposits of mortar. All dust was removed using an air hose. This was done to ensure excellent adhesion between the block and the fabric. Surface preparation is very important to the success of FRP application because any irregularities can result in premature delamination [13]. The GFRP fabric was cut to cover an area equal to the length of the bed joint times 590 mm (three block heights plus two mortar bed joints). The GFRP was bonded to the specimens using a two-part epoxy provided by the manufacturer. The epoxy was applied to the surface of the specimens using a paint roller. The pre-cut sheets of glass fabric were then saturated with the epoxy and placed on the specimens. Several passes of the paint roller were used to remove excess epoxy and any air voids.

Since the specimens were not grouted there was concern that they might fail in compression at the supports rather than by shear-slip along the bed joints. This would diminish the value of the test. Therefore, to help ensure shear-slip failure along the bed joints the block cells at the “head” and “feet” of each specimen were grouted and subsequently wrapped with GFRP. Before the specimens were tested, the epoxy was allowed to cure for at least five days. Prior to testing, the top and bottom of each specimen was capped with a thin layer of Hydrostone to ensure full contact with the 12.7 mm (½ inch) thick steel loading plates.

TEST SETUP AND INSTRUMENTATION

The specimens were tested under monotonically increasing compression loading. The smaller specimens (i.e. A-0.5, A-1.5, T-1.0) were tested in a Tinius Olsen testing machine, as seen in Figure 2. For the larger specimens (i.e. A-2.5, T-3.0) it was necessary to construct a customized testing apparatus, as seen in Figure 3. The apparatus consisted essentially of two steel columns, a spreader beam and a 50 mm (2 inch) thick steel top bearing plate. The load was applied using a hydraulic cylinder, with a 1779 kN (400,000 lbs.) maximum capacity. The load was monitored using a commercial load cell.



Figure 2 – Test of Smaller Specimens Using Test Machine



Figure 3 – Test of Larger Specimens Using Customized Testing Apparatus

Specimens placed in either testing apparatus were positioned and centred as perfectly as possible to limit any rotation of the blocks in the direction perpendicular to the plane of the laminate. For the smaller specimens (i.e. A-0.5, A-1.5, T-1.0) the relative movement across the bed joint slip planes was measured using a mechanical gauge. For the T-1.0 specimens the mechanical gauge was oriented vertically and parallel to the bed joint and spanned the middle gap. Measurements were taken along both bed joints. For the A-0.5 and A-1.5 specimens this gauge was oriented at an angle across the bed joint. The angle was so small that that any displacement was assumed to equal that parallel to the bed joint. Once again measurements were taken along both bed joints. The nominal gauge length was 200 mm. For the larger specimens (i.e. A-2.5, T-3.0) the relative movement between the blocks along the slip plane was measured using 25 mm linear potentiometric displacement transducers (LPDTs) connected to a PC data acquisition system. For the T-3.0 specimens four LPDTs were placed vertically and parallel to the bed joints and spanned the middle gap. For the A-2.5 specimens, using extension arms to cross the bed joint, four LPDTs were placed vertically and parallel to the bed joints. For the T-3.0 and A-2.5 specimens the nominal gauge lengths were 1200 mm and 995 mm, respectively.

For the smaller specimens (i.e. A-0.5, A-1.5, T-1.0) the load was recorded manually from the dial on the machine. For the A-2.5 and T-3.0 specimens the load was recorded using a commercial load cell, which was also connected to the data acquisition system. For the specimens with GFRP a 445 kN (100,000 lbs.) load cell was used. Because the specimens without GFRP would fail at much lower loads, a 111 kN (25,000 lbs.) load cell was used for improved resolution.

EXPERIMENTAL RESULTS

Failure of the unretrofitted specimens was a brittle shear-slip debonding mode that occurred at low levels of both load and displacement. The debonding occurred at the interface between the block and the mortar, as shown in Figure 4. This failure mode is typical considering the weak shear bond strength of the mortar and the absence of compressive stresses normal to the mortar

bed joints for these tests. Previous investigations [6, 7] have documented the strengthening and deformational benefits of axial compression. This type of failure mode is very brittle and as described by Hamid et al. [10], very little time elapsed between the initiation of cracking at the block-mortar interface and total debonding.

All of the reinforced specimens, with one exception, failed in shear slip along the bed joints but at much higher loads. As shown in Table 2, they reached shear slip strengths ranging from 3.2 to 7.7 times that of their unretrofitted counterparts. Upon examining the failed specimens it was discovered that the mortar joints were damaged and thus the laminates were resisting the entire applied load. For all of the retrofitted specimens, at large slip displacements, the laminate became entirely torn, as shown in Figures 5 and 6, and could not resist further loading. Failure by delamination did not occur with any of the specimens. The exception to the above description was specimen type AR-2.5 which consistently failed by toe crushing. The laminate was undamaged and, therefore, the strength is only a lower bound estimate of shear-slip capacity.



Figure 4 – Unretrofitted



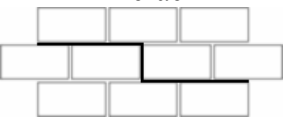
Figure 5 – GFRP Failure

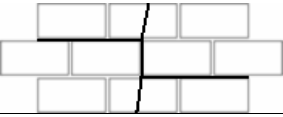
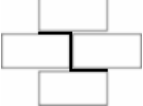
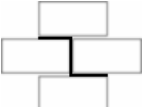
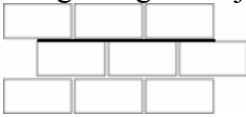
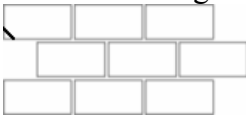
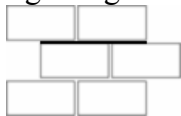


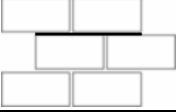
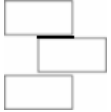
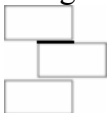
Figure 6 – GFRP Failure

The complete summary of the shear slip strengths and typical failure modes is found in Table 2. As can be seen, the unreinforced specimens exhibited high variability (measured by the COV). For all of the specimens the application of the GFRP greatly reduced the variability

Table 2 - Phase 1 Typical Failure Modes & Failure Loads

TU – 3.0 (Unreinforced)				
Typical Failure Mode	Specimen	Failure Load (kN)	Shear Strength (MPa)	C.O.V. %
<p style="text-align: center;">‘Z’ crack</p> 	1	22.8	0.29	15.3
	2	27.9	0.35	
	3	28.8	0.36	
	4	31.0	0.39	
	5	21.6	0.27	
	Average	26.4	0.33	

TR – 3.0 (Reinforced)				
Typical Failure Mode	Specimen	Failure Load (kN)	Shear Strength (MPa)	C.O.V. %
'Z' crack or 'Z' crack with middle block failure 	1	207.5	2.61	2.5
	2	205.2	2.58	
	3	197.7	2.48	
	Average	203.5	2.56	
	TU – 1.0 (Unreinforced)			
Typical Failure Mode	Specimen	Failure Load (kN)	Shear Strength (MPa)	C.O.V. %
'Z' crack 	1	12.4	0.49	21.6
	2	9.8	0.39	
	3	11.7	0.46	
	4	16.3	0.65	
	Average	12.5	0.50	
TR – 1.0 (Reinforced)				
Typical Failure Mode	Specimen	Failure Load (kN)	Shear Strength (MPa)	C.O.V. %
'Z' crack 	1	37.5	1.49	6.4
	2	39.6	1.58	
	3	42.6	1.69	
	Average	39.9	1.59	
	AU – 2.5 (Unreinforced)			
Typical Failure Mode	Specimen	Failure Load (kN)	Shear Strength (MPa)	C.O.V. %
Cracking along a bed joint 	1	43.4	0.32	20.5
	2	49.9	0.37	
	3	56.6	0.42	
	4	42.7	0.32	
	5	31.8	0.24	
	Average	44.9	0.33	
AR – 2.5 (Reinforced)				
Typical Failure Mode	Specimen	Failure Load (kN)	Shear Strength (MPa)	C.O.V. %
Toe crushing 	1	232.2	1.72	16.1
	2	168.2	1.24	
	3	197.0	1.46	
	Average	199.1	1.47	
	AU – 1.5 (Unreinforced)			
Typical Failure Mode	Specimen	Failure Load (kN)	Shear Strength (MPa)	C.O.V. %
Cracking along a bed joint 	1	13.8	0.17	24.7
	2	22.5	0.28	
	3	27.6	0.34	
	4	27.6	0.34	
	5	23.0	0.28	
	Average	22.9	0.28	

AR – 1.5 (Reinforced)				
Typical Failure Mode	Specimen	Failure Load (kN)	Shear Strength (MPa)	C.O.V. %
Cracking along a bed joint 	1	137.0	1.69	1.0
	2	135.0	1.67	
	Average	136.0	1.68	
	AU – 0.5 (Unreinforced)			
Typical Failure Mode	Specimen	Failure Load (kN)	Shear Strength (MPa)	C.O.V. %
Cracking along a bed joint 	1	2.1	0.08	72.0
	2	8.8	0.33	
	3	3.7	0.14	
	Average	4.8	0.18	
AR – 0.5 (Reinforced)				
Typical Failure Mode	Specimen	Failure Load (kN)	Shear Strength (MPa)	C.O.V. %
Cracking along a bed joints 	1	30.0	1.13	18.0
	2	27.0	1.02	
	3	38.0	1.43	
	Average	31.7	1.19	

An average face shell thickness of 34 mm was used in calculating shear stress for both reinforced and unreinforced specimens. As can be seen in Table 2, two distinct failure modes can be seen. For the triplet type of specimen, only one side of the specimen failed whereas, for the modified triplet type specimens, cracks and failure occurred above and below the empty head joint on opposite sides of the specimen. For this type of specimen, it was not possible to have only one side fail because any “softening” of the response on one side of the specimen results in a shifting of load to the other side.

Typical load versus displacement behaviour of the unreinforced specimens can be seen in Figure 7, for specimen TU-3.0. These specimens exhibited a sudden, brittle loss of capacity for their maximum stress at an average slip of 0.051 mm. In comparison, after retrofitted assemblages reached their respective maximum loads, a gradual decrease in load occurred, as shown in Figure 8, for specimen TR-3.0. This greatly increased deformability and ended with the eventual tearing of the GFRP laminate. The experimental and analytical work conducted by Ehsani et al. [1] revealed that when FRP fibres were oriented at 0°/90° to the applied load, the resulting shear-deformation relationship was nonlinear. This was shown to be the case here.

For the illustrated specimens, the average shear slip displacement at the maximum shear stress was 0.772 which is in excess of 15 times that of its unretrofitted counterpart. The average maximum displacement was 6.6 mm.

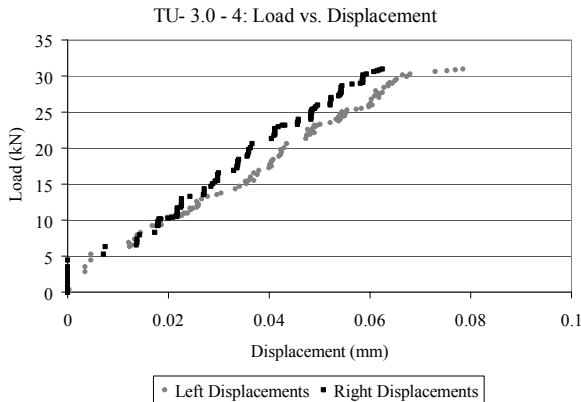


Figure 7 – Load-Displacement Data for Specimen TU-3.0

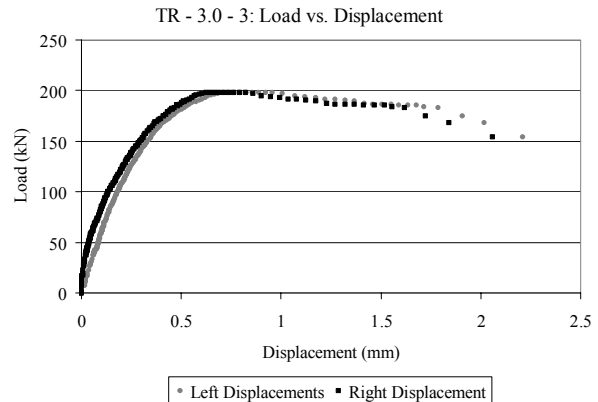


Figure 8 – Load-Displacement Data for Specimen TR-3.0

SELECTION OF SPECIMEN CONFIGURATION

In evaluating the various shapes of the test specimens, several factors have been considered. In general, the single triplet (type ‘A’) shape of specimens introduces more bending stresses over the length of the bed joint due to unavoidable eccentricity of the positions of the applied load and reaction points. Although this bending could be substantially reduced by applying the loads close to the bed joints and similarly locating the reactions close to the other side of this slip plane, some bending remains. Also, for the specimens with longer slip planes, compression failure at the toe due to reaction forces near the bed joint made such specimens unsuitable for the study.

In terms of the distribution of shear stress along the bed joint, a finite element analysis by Atkinson et al. [7] showed that nearly uniform stress exists except near the ends of the shear transfer zone. Therefore, use of a longer shear transfer zone reduces the impact of this region of nonuniform stress. The finite element analysis also showed that the modified triplet (type ‘T’) shape of specimen inherently produces a more nearly pure shear conditions along the bed joint slip plane. This shape of specimen also, typically, had less variability of results. Therefore, the T-type was preferable.

Considering both the need to minimize bending stress normal to the bed joint and the desire to have uniform shear stresses, the T-3.0 type of specimen has been chosen for further shear slip research.

CONCLUSION

Thirty-six shear-slip assemblages were tested in direct shear to select a specimen configuration for the next phase of this experimental investigation. As indicated above, the T-3.0 specimen was chosen as providing the best combination of minimal bending stress, uniform shear stress and limited variability of results. The following additional information was acquired:

1. GFRP laminates significantly increase the load carrying capacity of URM. The retrofitted specimens reached shear slip strengths ranging from 3.2 to 7.7 times that of their non-retrofitted counterparts.
2. Masonry assemblages retrofitted with GFRP exhibited ductile failure and much greater maximum displacements before failure.
3. GFRP laminates reduce the variability of URM.

ACKNOWLEDGEMENTS

Special thanks go to Edward Fyfe and Peter Milligan of Fyfe Co. LLC, California for their generous donation of the GFRP, the Ontario Masonry Contractors' Association and the Canada Masonry Design Centre for the mason's time, and the Ontario Concrete Block Association for the concrete blocks. The financial support for this research from the ORDCF funded Centre for Effective Design of Structures at McMaster University is gratefully acknowledged.

REFERENCES

1. Ehsani, M. R., Saadatmanesh, H., Al-Saidy, A. "Shear Behavior of URM Retrofitted with FRP Overlays." *Journal of Composites for Construction*. Vol. 1, No. 1, 17 – 25. 1997.
2. Hall, J. D., Schuman, P. M., Hamilton III, H. R. "Ductile Anchorage for Connecting FRP Strengthening of Under-Reinforced Masonry Buildings." *Journal of Composites for Construction*. Vol. 6, No. 1, 3 – 10. 1997.
3. Mangenes, G., Calvi, G. M. "In-plane Response of Brick Masonry Walls." *Earthquake Engineering Structural Dynamics*, 26, 1091 – 1112. 1997.
4. Drysdale, R. G., Hamid, A. A., Baker, L. R. *Masonry Structures: Behavior and Design (2nd ed.)*. The Masonry Society, Boulder, Colorado. 1999.
5. Applied Technology Council (ATC-33 Project). "NEHRP Commentary on the Guidelines for the Seismic Rehabilitation of Buildings." *FEMA Publication 274*. Washington, D.C. 1997.
6. Drysdale, R. G., Vanderkyle, R., Hamid, A. "Shear Strength of Brick Masonry Joints." Proceedings of the Fifth International Brick Masonry Conference, Washington, D.C. 1979.
7. Atkinson, R. H., Amadei, B. P., Saeb, S., Sture, S. "Response of Masonry Bed Joints in Direct Shear." *Journal of Structural Engineering*. Vol. 115, No. 9, 2276 – 2296. 1998.
8. Canadian Standards Association. "Masonry Design for Buildings." CSA S304.1-04, CSA, Mississauga, Ontario. 2004.
9. Triantafillou, T. C. "Strengthening of Masonry Structures Using Epoxy-Bonded FRP Laminates." *Journal of Composites for Construction*. Vol. 2, No. 2, 96 – 104. 1998.
10. Hamid, A. A., El-Dakhkhni, W. W., Hakam, Z. H. R. "Behavior of Composite Unreinforced Masonry – Fiber-Reinforced Polymer Wall Assemblages Under In-Plane Loading." *Journal of Composites for Construction*. Vol. 9, No. 1. 2005.
11. Harris, H. G., Sabnis, G. M. *Structural Modeling and Experimental Techniques (2nd ed.)*. CRC Press, New York. 1999.
12. Fyfe Co. LLC [online] 2004,
Available: <http://www.fyfeco.com/products/compositesystems/web.html>
13. Abdel-Wahed, O. H. "Application and Rehabilitation of FRP in Masonry Wall." Research Submitted for the Requirement of the Degree of Full Professor in Structural Engineering. Ain Shams University, Cairo, Egypt. 2004.